Computational Investigation of Aqueous Droplets containing Environmentally Relevant Molecules

Adeniyi Olajide

A Thesis
In the Department
of
Chemistry and Biochemistry

Presented in Partial Fulfillment of the Requirements
For the Degree of
Master of Science (Chemistry)
Concordia University
Montreal, Quebec, Canada

April, 2022

CONCORDIA UNIVERSITY

SCHOOL OF GRADUATE STUDIES

This is to certify that the thesis prepared

By: Adeniyi Olajide

Entitled: Computational Investigation of Aqueous Droplets containing Environmentally Relevant Molecules

and submitted in partial fulfillment of the requirements for the degree of

Master of Science (Chemistry)

complies with the regulations of the University and meets the accepted standards with respect to originality and quality.

Signed by the final Examining Committee:

Dr. Louis Cuccia Examiner

Chair's name

Dr. Dajana Vuckovic Examiner

Examiner's name

Dr. Yves Gelinas Examiner

Examiner's name

Dr. Gilles Peslherbe Supervisor

Supervisor's name

Approved by _____

Dr. Yves Gelinas (Graduate Program Director)

_____2022 _____

Dr. Pascale Sicotte,
Dean of Arts and Sciences

Abstract

Computational Investigation of Aqueous Droplets containing Environmentally Relevant Molecules

Adeniyi Olajide

The abundance of aqueous ions plays a significant role in various processes, including environmental ones such as cloud condensation nucleation. The details of ion-water and water-water interactions are critically important in these processes and require further insights from molecular simulations. Towards elucidating the hydration of ions in clusters, molecular dynamics (MD) simulations based on first-principles, implementing the density-functional tight-binding model with the third-order expansion (DFTB3), were employed to predict the properties of water clusters of varying sizes seeded with polyatomic ions (ClO_x^- and NO_x^-). Validating the predictions of the DFTB3 model against high-level quantum chemistry data established the robustness and accuracy of DFTB3 in evaluating small cluster properties of ClO_x^- $(H_2O)_n$ and NO_x^- $(H_2O)_n$. In order to enhance conformational sampling of the clusters, a parallel tempering approach of MD simulations was implemented, and the potential of mean force (PMF) along the ion to water cluster center-of-mass distance was calculated by implementing umbrella sampling in the DFTB3-MD simulations. On the basis of the probability distributions of the ions with respect to the water cluster moiety center of mass obtained from the PMF, it appears that ClO_x^- and NO_x^- ions exhibit surface behaviour in water clusters, with the larger oxides showing more preference for surface solvation. This feature may influence the chemistry of the ions as they will be readily available for reactions with other atmospheric particles.

Acknowledgments

Foremost, I would like to express my heartfelt gratitude to my supervisor, Prof. Gilles Peslherbe, for his unwavering support towards my Master's program research, as well as his patience, motivation, and enthusiasm. His advice was invaluable in my research and writing of this thesis.

Aside from my advisor, I'd like to thank the other members of my thesis committee: Prof. Yves Gelinas and Prof. Dajana Vuckovic, for their encouragement, insightful comments, and difficult questions.

I would like to thank Dr. Denise Koch for helping out with codes despite her tight schedules. I appreciate CERMM Group colleagues for the stimulating discussions and good times we had.

Finally, I would like to thank my family for their patience and support throughout the program.

Dedication

This thesis is dedicated to all graduate students struggling with their research. Keep your hopes high.

Table of Contents

List of Figures

List of Tables

List of Abbreviations

AIM	Atoms in Molecules
B3LYP	Becke, 3-parameter, Lee–Yang–Parr
BCP	Bond Critical Point
CCSD(T)	Coupled Cluster with Single, Double and perturbative Triple excitations
DFT	Density-Functional Theory
DFTB3	Density-Functional Tight-Binding with 3rd order expansion
KS	Kohn Sham
LANS	Large-angle Neutron Spectroscopy
LAXS	Large-angle X-ray Scattering
MBL	Marine boundary layer
MD	Molecular Dynamics
MP2	Second-order Møller–Plesset perturbation theory
NVE	Particle Number, Volume and Energy
OB	Parameter set for Organic and Biological molecules
P	Probability
PMF	Potential of Mean Force
QTAIM	Quantum Theory of Atoms in Molecules
REMD	Replica Exchange Molecular Dynamics
SOA	Secondary Organic Aerosols
U	Potential Energy
WHAM	Weighted Histogram Analysis method

Chapter 1

Introduction

1.1. Solvation

Solvation is one of the most essential and highly researched topics in physical chemistry.[1–4] Basically, solvation involves the (re)arrangement of solvent molecules around a solute. Depending on the nature of the dipole-dipole and ion-dipole interactions in the solute-solvent system, there is a resulting change in the system's physical properties. Owing to the ubiquity of water molecules, the most common solvation type is hydration.

Water molecules interacting directly with the solute form a so-called hydration sphere, whereas the neighboring water molecules interacting with the first hydration sphere water molecules form the second hydration sphere. The first two hydration spheres are of great significance as they affect the structure and functions of the solute.[5]

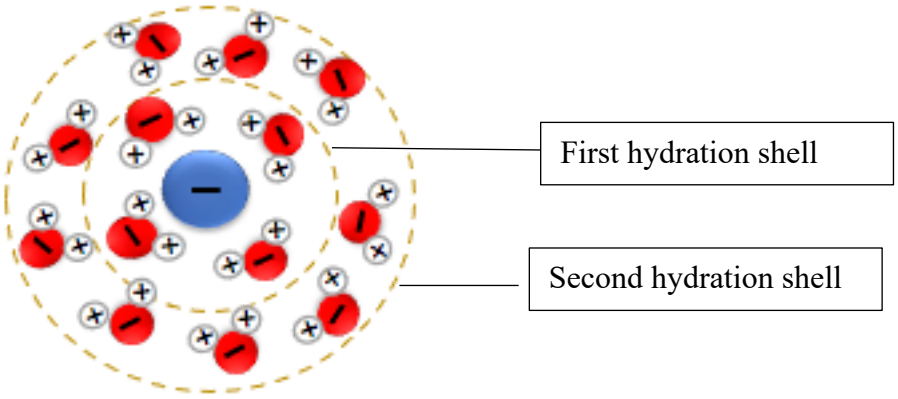

Figure 1. Schematic picture of the hydration shell of an anion

The behaviour of water clusters is greatly impacted by temperature. Hence, the thermodynamic properties of water clusters differ from the bulk properties. Although, cluster melting temperature has been attributed to cluster size,[6] the phase behavior of water clusters is still debatable and requires further insight to include the roles of ions present in the cluster.

Hydrogen bonding is the dominant bonding interaction in water clusters and it dictates their physical and chemical properties. The formation and breakage of hydrogen bonds in water clusters occur very quickly and this fluxional feature is important in the analysis of the behavior of aqueous solvation shells around solutes. Besides experimental studies, a detailed understanding of water clusters will require theoretical investigations, possible using molecular modeling and simulations.

1.2. Aqueous Ions in Water Clusters

Ions can be classified as structure maker[7,8] or structure breaker depending on the nature of their interactions with water molecules. For instance, the interaction of an ion with immediate neighboring water molecules can be stronger or weaker than those in bulk water. Disruptions of the water cluster bonding network caused by ions initiate a rearrangement of the cluster structure. This process helps accommodate the ion and results in the breakage of hydrogen bonds. Ion-water hydrogen bonds formed compensate for the loss of water-water hydrogen bonds. The ion-water interaction is dependent on the strength and number of hydrogen bonds formed when the ion is solvated.

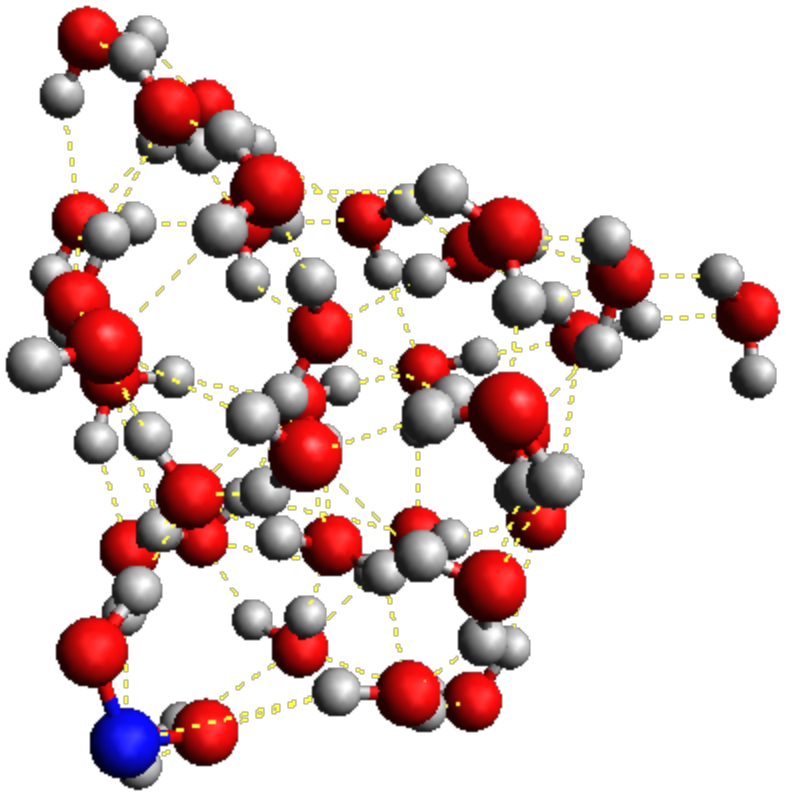

Figure 2. Hydrogen bonding interactions between water molecules and ion

Detailed knowledge of solvated anions is confined to a few species, in particular simple ionic species. The hydration of monovalent monoatomic anions[9] and metallic cations[10,11] have been well investigated. However, the hydration of polyatomic anions becomes more complex as the charge is no longer uniformly distributed.

1.3. Marine Boundary Molecular Ions

Marine boundary layer (MBL) aerosols containing inorganic salts are the result of turbulent wave action at the ocean's surface. Atmospheric particulate matter contains high amounts of chloride and nitrogen oxide aerosols which play significant roles in atmospheric chemistry.[12] However,

their impact on the nucleation of atmospheric particles is not well understood. The molecular reaction between the chloride ion and ozone which leads to the formation of oxychloride anions is a major concern in the decomposition of ozone.[13,14]

Chlorine exists in oxidation states higher than -1 in oxychloride anions, and most of the homologous members of this oxychloride anion family have been reported to be present in substantial amounts in aerosols.[15] As for nitrogen oxide species, Jungwirth and co-workers[16] first predicted the surface propensities of nitrate, which was later contradicted in the reports of Dang and co-workers[17], stating that the probability of finding nitrate at aqueous interfaces is low.

Owing to the high abundance of atmospheric water molecules, the nature of the interactions between molecular ions and water molecules is essential for answering existing questions related to atmospheric chemistry. Detailed information concerning the hydration of oxychloride and nitrogen oxide anions has not been clearly elucidated.

1.4. Computer Simulation of Ion-Water Droplets

The complex nature of ion solvation necessitates the application of robust techniques to ensure a detailed analysis of the structural and dynamical features of ion-water clusters.

The true power of computational chemistry resides in the expansion of static property calculations to dynamical behavior simulation. For this objective, molecular dynamics (MD) simulation is an excellent choice. MD simulation is a versatile technique that can be applied to generate ensembles of structures for further analysis. It has been an effective method for modeling ion-water clusters.[18,19] MD simulation is based on an algorithm that predicts atomic positions based on a small increment of time (time step, δt) given their initial values. This is achieved by integrating the forces on nuclei to obtain their velocities. Consequently, the positions of the nuclei are updated. A widely implemented algorithm for this purpose is the velocity Verlet algorithm.[20] In the latter,

the position of the particles is approximated one step in the future from the present time using a Taylor series approximation. This approach predicts the atomic positions of the system at time t + δt based on the current position (r), velocities (v), atomic mass (m) and forces acting on the atoms (F). The equations to calculate the successive timesteps using the velocity Verlet algorithm are given as:

$$r(t + \delta t) = r(t) + v(t)\,\delta t + \frac{1}{2m} F(t)\delta t^2, \tag{1.1}$$

$$v(t + \delta t) = v(t) + \frac{F(t) + F(t + \delta t)}{2m}\delta t. \tag{1.2}$$

It is possible to sample microcanonical ensembles (NVE) by integrating the equations of motion using the standard Verlet integration. However, when constant temperature is involved, a heat bath coupling such as the Nose-Hoover thermostat[21] is implemented to regulate the temperature.

Classical molecular dynamics simulation which makes use of force fields is quite common due to the wide applicability and suitability for large systems owing to its moderate demand on computational resources. A force field is a mathematical description that models the interactions of atoms and molecules at the atomic and molecular levels. The force field captures the essential intra and intermolecular interactions responsible for the relative potential energy of the possible conformations as well as intermolecular arrangements of molecules. The applications of force fields are limited as they do not explicitly include electrons in the calculations and as such are unable to describe the chemistry of bond formation and breakage in systems.

The limitation of force fields mentioned above can be overcome by implementing *ab initio* molecular dynamics methods but the major set-back with the required *ab initio* quantum chemistry calculations lies in their high computational cost, which increases exponentially with the system size.

1.4.1. Replica Exchange Molecular Dynamics (REMD) Simulations

Achieving realistic canonical distributions with conventional simulation approaches is particularly challenging at low temperatures because simulations at low temperatures tend to get trapped in one of a large variety of local minimum-energy states, especially when dealing with systems of high fluxionality such as water clusters.

REMD simulation is one technique used to avoid the multiple-minima problem. It enables breaking through any energy barrier and more efficient exploration of the phase space than conventional methods. Several replicas of the system are run in parallel at different temperatures and then swapped periodically according to a Metropolis-Hastings criterion:[22]

$$A = \min\{1, e^{(\beta_i - \beta_j)(U_i - U_j)}\}, \tag{1.3}$$

where A represents the probability of exchange between the i-th and j-th conformations, U is the conformation potential energy and ß =1/k_BT (k_B is the Boltzmann constant and T is the temperature).

1.4.2. Umbrella Sampling and Potential of Mean Force

Chemical processes are characterized by free energy.[23] The difference in free energy between two states determines the probability of finding a molecular system in one of those states. As a result, free-energy differences can be linked to a variety of fundamental chemical parameters, including binding constants, solubilities, partition coefficients, and adsorption coefficients.[24] For these

reasons, one of the most important tasks for a computational chemist is to calculate free energies accurately, particularly the free energy profile along a chemical or biological process.

In canonical MD simulations, the Boltzmann distribution of states is sampled, and the probability (P) that the solute will be situated at position r is dependent on the potential energy (U) of that configuration:

$$P_{(r)} \propto exp\left(\frac{U_{(r)}}{RT}\right) \tag{1.4}$$

Higher energy configurations will only be sampled seldom since the probability of a state being sampled reduces exponentially with its potential energy. Therefore, higher energy portions of the free energy profile may not be sufficiently sampled with a conventional MD simulation. Thermodynamic integration, perturbation theory, and umbrella sampling are some of the free energy calculation approaches developed in recent decades.[25–27]

Umbrella sampling is widely used for calculating the potential of mean force (PMF) i.e. the free energy change along a given coordinate. The reaction coordinate in umbrella sampling is restrained to a target value by a bias potential according to the expression:

$$U_{umb,i}(r) = \frac{1}{2}k(\mathrm{z} - z_{0,i})^2, \tag{1.5}$$

where k is the spring constant and $x_{0,i}$ is the reference position of the restraint. Typically, umbrella sampling is implemented as a succession of windows, which are then combined using the weighted histogram analysis method (WHAM)[28] in order to remove the bias potential.

In this thesis, the hydration extent of the molecular ions is analysed in terms of the probability distribution $P(r_{cm})$ of the distance between the ion and water cluster centers of mass r_{cm} calculated from the corresponding PMF. The PMF is related to the spatial probability distribution along a reaction coordinate $p(\xi)$ according to this expression:[25]

$$\Delta F = -k_B T ln\langle p(\xi)\rangle , \tag{1.6}$$

where the PMF is denoted by ΔF.

1.5. Electronic Structure

Electronic structure theory considers the motion of electrons. Basically, properties of a system can be solved with the time-independent Schrodinger equation:

$$\hat{H}\Psi = \hat{E}\Psi , \tag{1.7}$$

where $\hat{H}$ is the Hamiltonian operator , Ψ is the wave function of the quantum system and $\hat{E}$ is the energy of the system. There is no exact analytical solution for systems other than the hydrogen atom as the solution becomes complicated with size. This necessitates the incorporation of various approximations into equation 1.7.

High-level quantum chemistry calculations such as the coupled cluster theory with single, double and perturbative triple excitations [CCSD(T)],[29] Second-order Møller–Plesset perturbation

(MP2) theory[30] and density-functional theory (DFT), with an exchange-correlation functional such as B3LYP (Becke, 3-parameter, Lee-Yang-Parr),[31] are known for their high degree of accuracy. These theories are used for the validation of the implemented methodology in this research.

Density-Functional Tight Binding (DFTB) model

Density-functional theory (DFT)[32–34] has proven to be highly useful in the theoretical description of the properties of electronic systems of atoms. This has been a development since the demonstration by Kohn and Hohenberg[35] of the theoretical grounds for density-functional theory, indicating that the energy of any electronic system is a universal functional of the electronic density ρ. According to the Kohn-Sham (KS) formulation, the energy of the many interacting electrons system is equal to that of a hypothetical system of independent electrons within an effective potential including nuclei interaction complemented by the electron-electron Coulomb interaction and exchange-correlation effects. Even though DFT exhibits favorable computational adaptations, there is always a need for more efficient techniques. This is particularly important when large systems are being modeled in the nanoscale domain as in molecular dynamics simulations, with the aim of reaching statistical convergence.

The density-functional tight-binding (DFTB) method is an approximate Kohn-Sham density-functional theory (KS-DFT) scheme with a Linear Combination of Atomic Orbital (LCAO) representation of the KS orbitals, and it has been applied for a large variety of problems in chemistry. DFTB is useful in many ways: (i) its computational scaling is less cumbersome, (ii) it is suitable for calculations of large systems, and (iii) it is suitable for extensive studies and dynamical properties of systems. The method retains key DFT features while offering the

computational speed of traditional semiempirical quantum chemistry approaches without the need for a large number of empirical parameters.

The derivation of the DFTB energy from the expansion of the KS total energy in terms of charge density fluctuations around a reference electron density has been well documented[36–38] and in this chapter, the emphasis will be on the final equations. The zeroth-order non-self-consistent-charge approach which is also referred to as the standard DFTB is obtained from zero-order expansion as:[39,40]

$$E^{DFTB0} = \sum_{i}^{occ} \langle \Psi_i | \hat{H} | \Psi_i \rangle \; + \; E^{rep} \, , \tag{1.8}$$

where E^{DFTB0} represents the electronic energy and E^{rep} is a sum of short-range repulsion potentials. The single-electron wave functions are represented as linear combinations of Slater-type orbitals, and the Hamiltonian operator is built based on a particular reference density. The expansion of the DFTB energy up to the third-order provides better results for systems containing charged atoms.[41]

$$E^{DFTB3} = \; E^{DFTB0} + \frac{1}{2} \sum_{ab} \gamma_{ab} \, \Delta q_a \Delta q_b + \frac{1}{3} \sum_{ab} \Gamma_{ab} \, \Delta q_a^2 \, \Delta q_b \, , \tag{1.9}$$

where γ_{ab} , the second order kernel, is a function that describes the extent of electron-electron interaction, while Δq_a and Δq_b are atomic charge fluctuations obtained from the Mulliken scheme in a self-consistent manner and the function Γ_{ab} represents the derivative of γ_{ab} with respect to charge variation.

1.6. Scope of the Thesis

The thesis is focused on understanding the interplay between solute-solvent and solvent-solvent interactions in fundamental hydration processes by implementing computer simulations capable of supplementing experimental studies.

The second and third chapters of this thesis open up with the validation of a suitable methodology for simulating environmentally-relevant molecular species such as oxychlorides and nitrogen oxide anions, respectively. The chapters then address implementation of the validated methodology to investigate the dynamical properties of water clusters containing the aforementioned environmentally-relevant molecular species.

Chapter 2

Microsolvation of Oxychloride Anions: Structural and Energetic Properties

2.1. Introduction

The universal nature of aqueous ions is a predominant feature that has been noticed over the years. The basic understanding of aqueous solutions containing charged species is quite pertinent to scientific and practical interests.[9] Structures and energetic properties of aqueous systems containing ions have been widely studied,[42–45] owing to their fundamental roles in myriads of processes. [10,46,47]

Ionic species' proclivity at the air-water interface might influence gas uptake and chemical interactions with liquid droplets in the lower troposphere, especially in the marine boundary layer. Simple ions such as alkali metals and halides have received considerable research focus,[48,49] and extensive studies have been carried out to understand their hydration phenomenon. Polyatomic anions, on the other hand, having non-uniform charge distribution, exhibit different hydration behaviour from those seen in simple ions. The commonly investigated polyatomic anion which has a high concentration in the marine boundary layer is sulphate (SO_4^{2-}).[50] Little attention has been drawn to anionic forms of chlorine oxides which have been reported to be players in atmospheric aerosol formation.[15] Oxychlorides are products of the reaction between ozone and the highly abundant atmospheric chlorine.[13,14]

Even though the major roles of these ions in atmospheric processes have not been well established, their hydration phenomenon may provide useful information, owing to the high fraction of such atmospheric water droplets. In order to investigate complex systems such as clusters of water molecules with an ion, it is best to understand the properties of increasing-size building blocks or small fragments of such systems. This systematic bottom-up approach helps to understand ion hydration, by step-wise addition of water molecules. Additionally, this approach can help comprehend the bulk properties of the aqueous system.

Various experimental and theoretical investigations have been carried out in order to understand the mechanism of ion hydration. Typically, commonly used experimental techniques such as large-angle X-ray scattering (LAXS)[51] and the large-angle neutron scattering (LANS)[52] are capable of accounting for long-range interactions resulting from the ion-water H-bonding. However, the fast exchange dynamics of the existing hydrogen bonding network between aqueous ions and the hydrating water molecules is a challenge for most experimental techniques.[53]

Theoretical techniques based on molecular dynamics (MD) simulations have proven to bridge the gap between theory and experiment by providing detailed information at the molecular level that could help understand the structure of water clusters.[18,54,55] In principle, molecular dynamics simulations can be employed to generate conformations from the time evolution of the system. Basically, most molecular simulation techniques rely on the description of interatomic interactions based on classical mechanics. The major setback to these techniques is their inability to account for breaking and formation of interatomic covalent bonds. In order to circumvent this, the effect of quantum mechanics is incorporated into the simulations.

While high-level quantum chemistry calculations produce results comparable with experiments, the computational cost involved with such calculations can be of great concern as the

number of electrons in the system increases. The density-functional tight-binding (DFTB) model is an approximate method based on density-functional theory that has been recently considered to be a suitable bridge between semiempirical methods and high-level quantum chemistry calculations, as an acceptable compromise between computational speed and accuracy of calculated results.

In the present study, we validated the DFTB method by showing the reproducibility of high-level quantum chemistry calculation results with the third-order extension of the density-functional tight-binding (DFTB3) model by examining the various possible structural and energetic properties of $ClO_{1-4}^{-}(H_2O)_{1-4.}$ The DFTB method is an approximate quantum chemistry method based on the Taylor expansion of the Kohn-Sham total energy in terms of charge density. This method involves choosing a reference density ρ_0 as a superposition of neutral atomic densities ρ_0^{α} and expanding the DFT exchange correlation functional up to the second order. A minimal basis set is used to evaluate the Hamiltonian matrix elements.

The properties of ion-water clusters are first studied with regard to the variation in the oxidation state of the solute species. In the latter part of the research, the structures and dynamical features of ion-water clusters containing 32 and 64 water molecules are investigated by implementing an enhanced sampling methodology known as replica-exchange molecular dynamics simulations.

2.2. Computational Details

High-level quantum-chemistry calculations were carried out with the coupled cluster with single, double and perturbative triple excitations [CCSD(T)] theory[29], second-order Møller–Plesset (MP2) theory[56] and density-functional theory (DFT)[34] using the B3LYP exchange-correlation functional,

together with Dunning's aug-cc-pVTZ correlation-consistent basis set augmented with diffuse functions.

Geometries of clusters were optimized using MP2 theory, and harmonic vibrational frequencies were calculated to confirm that the obtained geometries correspond to local minima. Stepwise binding energies involved in the addition of an extra molecule of water were obtained from the zero-point energy (ZPE) corrected values using the expression:

$$\Delta E_{n,\,n-1} = E[X^-(H_2O)_n] - E[X^-(H_2O)_{n-1}] - E[H_2O], \qquad (2.1)$$

where X^- represents the polyatomic anions.

DFTB3 calculations were carried out using the 3OB Slater-Koster and third-order parameter sets.[57] The conjugate-gradient method was used for geometry optimizations, with a force threshold of 1×10^{-5}au.

Simulations of clusters containing oxychloride and 32 and 64 water molecules were performed using REMD-DFTB3. The velocity Verlet algorithm was used to integrate the equations of motion with a time step of 1 fs. The REMD simulation technique was incorporated to further enhance sampling efficiency by having a parallel tempering between 50 – 400 K with an increment of 50 K between two replicas. Exchange probability between two consecutive replicas were determined in correlation with Metropolis-Hastings criterion,[22] under the selected thermal condition. The systems were first equilibrated for 60 ps and the data collected for another 60 ps. In order to prevent water evaporation, spherical boundary conditions[58,59] were imposed, with a radius of 10 Å, which is quite larger than typical cluster radii by at least 3 Å. The umbrella sampling

method[25] was implemented to ensure efficient sampling while the weighted histogram analysis method (WHAM)[28] was used to remove biasing potentials.

The structural characteristics of the clusters are examined by means of the radial intermolecular ion-H probability distributions for $ClO_{1\text{-}4}^{-}(H_2O)_{32}$. Note that P(r) represents relative spatial probabilities and it differs by a factor of $4\pi r^2$ from the radial distribution function g(r) used in liquid structure theory.

$$\mathrm{P}(r) = \frac{\mathrm{dN_{coord}}(r)}{\mathrm{d}r} = \mathrm{n}\frac{4\pi r^2 g(r)}{\int_0^{\infty} 4\pi r^2\, g(r)\mathrm{d}r} \tag{2.2}$$

All quantum chemistry and DFTB calculations were performed using the Gaussian09 program[60] and DFTB+[61] package, respectively. The quantum theory of atoms in molecules (QTAIM) analysis was performed with the AIM2000 package,[62] and all simulations were performed with in-house MD codes.

2.3. Results and Discussion

2.3.1. Structural Properties and Bonding Topology of ClO_x^- (H_2O) [x = 1-4] Clusters

The optimized geometries of the ClO_x^- (H_2O) binary clusters are shown in Figure 3. Except for the ClO^- (H_2O) structure, which exhibit a planar geometry whereby the main hydrogen bonding occurs between one of the H atoms in the water molecule and the electron-rich O atom in the ClO^-, the rest of the binary cluster structures are stabilized by the interaction between two O atoms in the ion and two H atoms of the water molecule.

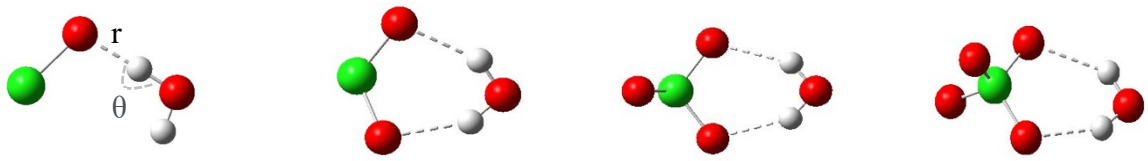

$ClO^-(H_2O)$ $ClO_2^-(H_2O)$ $ClO_3^-(H_2O)$ $ClO_4^-(H_2O)$

Figure 3. Optimized structures of $ClO_{1\text{-}4}^-(H_2O)$ binary clusters at MP2/aug-cc-pVTZ level

The geometric properties calculated from two levels of theory are shown in Table 1. The bond angle observed in the $ClO^-(H_2O)$ binary cluster has a larger magnitude than that for other binary clusters because the ionic species could not provide a bonding pair with the second H atom in the water molecule making the water molecule readily available for an interaction with a neighbouring molecule. As expected, the bond angle reduces with ion size. Generally, the bond angles predicted by DFTB3 slightly underestimate results from MP2.

Table 1. Selected geometric properties of binary clusters

Clusters	MP2/aug-cc-pVTZ	DFTB3/3OB
Bond angles (°)		
$ClO^-(H_2O)$	178.5	168.8
$ClO_2^-(H_2O)$	148.1, 148.1	147.0, 147.1
$ClO_3^-(H_2O)$	144.7, 145.0	143.6, 144.4
$ClO_4^-(H_2O)$	142.1, 145.2	141.0, 140.4
Δ		2.8
Bond Length (r) (Å)		
$ClO^-(H_2O)$	1.56	1.63
$ClO_2^-(H_2O)$	1.97, 1.97	1.93, 1.93
$ClO_3^-(H_2O)$	1.97, 2.11	1.94, 1.96
$ClO_4^-(H_2O)$	2.09, 2.13	2.04, 2.04
Δ		0.07

Δ is the absolute mean deviation of the DFTB data from MP2/aug-cc-pVTZ data

Calculated hydrogen bond lengths between the oxychloride ions and water molecule increase with ion size and vary inversely to the electron density at the bond critical points $\rho_{BCP}(r)$ predicted by QTAIM analysis (Figure 4). In addition, the magnitude of $\rho_{BCP}(r)$ values suggest that the H-bond strength decrease with ion size.

The molecular graphs of the binary clusters are shown in Figure 4. The Laplacian at the bond critical point $\nabla^2\rho(r)$ is positive, confirming the non-covalent nature of the interaction between the ion and water molecule.

a

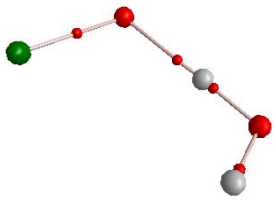

ρBCP (r) = 0.479 e/Å^3

$\nabla^2\rho(r)$ = 2.17 e/Å^5

b

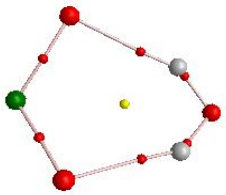

ρBCP (r) = 0.181 e/Å^3

$\nabla^2\rho(r)$ = 2.02 e/Å^5

c

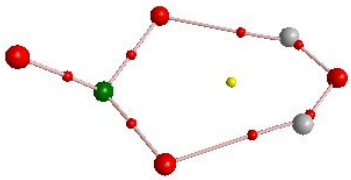

ρBCP (r) = 0.134 e/Å^3

$\nabla^2\rho(r)$ = 1.72 e/Å^5

d

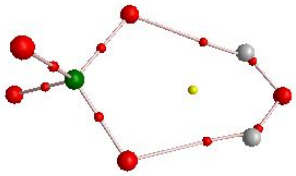

ρBCP (r) = 0.125 e/Å^3

$\nabla^2\rho(r)$ = 1.66 e/Å^5

Figure 4. Molecular graphs of $ClO_{1\text{-}4}^-(H2O)$ binary clusters (a) ClO^- (H_2O) (b) ClO_2^- (H_2O) (c) ClO_3^- (H_2O) (d) ClO_4^- (H_2O) showing electron densities and Laplacian values at selected bond critical point (BCP)

2.3.2. Binding Energies and Structural Motifs of Small $ClO_x^-(H_2O)_n$ [x = 1-4; n= 1-4, 6] Clusters

Table 2 displays stepwise binding energies of oxychloride-water clusters as a function of cluster size (n=1-4). The stepwise binding energies decrease as a function of cluster size and are generally lower with increasing chlorine oxidation number for oxychlorides; the relative binding strengths observed for the binary clusters are consistent with geometrical features of the cluster structures (elongation of intermolecular H-bonds with increasing chlorine oxidation number, Table 1). The DFTB3/3OB model reproduces the same trend as that obtained from CCSD(T) data.

Table 2. Stepwise binding energies of $ClO_{1-4}^-(H_2O)_{1-4}$ clusters

	$ClO^-(H_2O)_n$		$ClO_2^-(H_2O)_n$		$ClO_3^-(H_2O)_n$		$ClO_4^-(H_2O)_n$	
n	CCSD(T)	DFTB3	CCSD(T)	DFTB3	CCSD(T)	DFTB3	CCSD(T)	DFTB3
1	14.9	16.9	14.9	16.9	11.6	12.0	9.1	11.4
2	13.2	14.0	11.6	12.8	10.0	11.2	8.3	9.8
3	10.8	11.9	10.8	11.9	9.3	9.3	7.2	6.0
4	9.1	11.4	9.3	7.6	8.8	8.8	6.4	5.2
Δ		**1.6**		**1.5**		**1.3**		**2.5**

All values are in kcal/mol. Results from CCSD(T)//MP2/aug-cc-pVTZ and DFTB3/OB calculations. Δ is the absolute mean deviation of the DFTB data from CCSD(T)//MP2/aug-cc-pVTZ data.

Low-lying energy structures of $ClO_x^-(H_2O)_{1-4}$ clusters are presented in Figure 5. The striking feature of all cluster structures is the propensity of the water molecules to form water-water bonds rather than closely associate with the oxychloride anions.

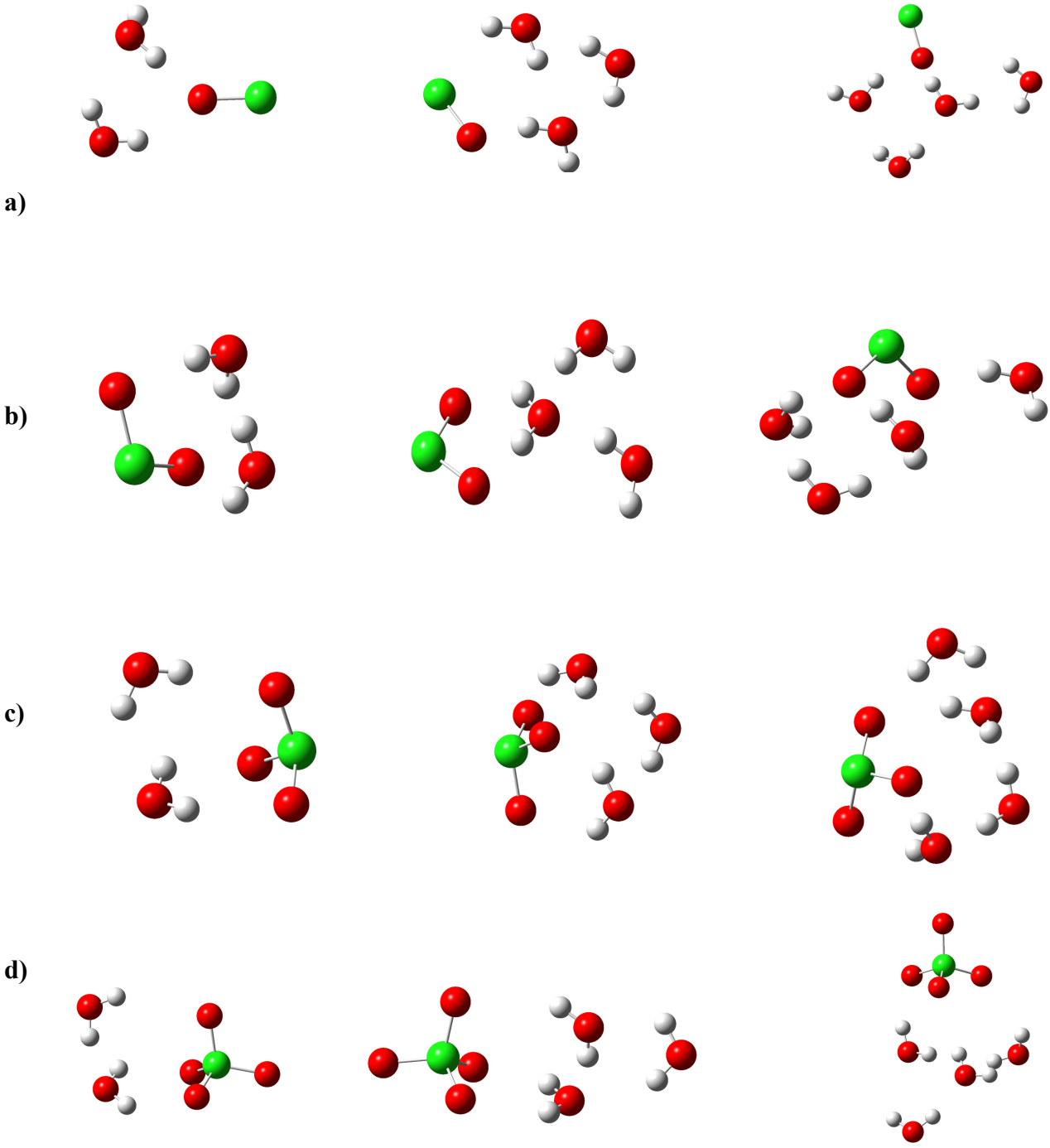

Figure 5. Optimized structures of (a) $ClO^-(H_2O)_{2-4}$ (b) $ClO_2^-(H_2O)_{2-4}$ (b) $ClO_3^-(H_2O)_{2-4}$ (c) $ClO_4^-(H_2O)_{2-4}$ predicted by MP2/aug-cc-pVDZ

Different minimum energy structures obtained from geometry optimization with the DFTB3 model for $ClO_4^-(H_2O)_6$ are displayed in Figure 6 alongside their calculated relative energies.

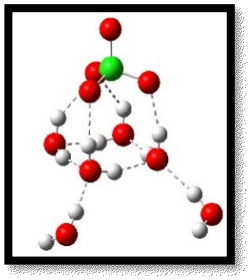

sm1

0 kcal/mol

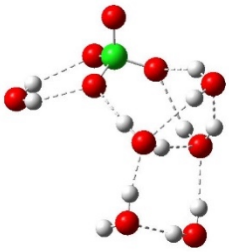

sm2

2.0 kcal/mol

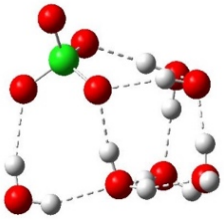

sm3

2.1 kcal/mol

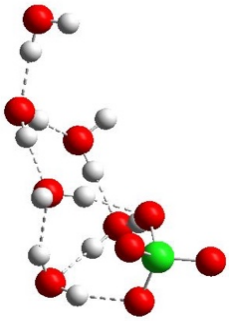

sm4

2.1 kcal/mol

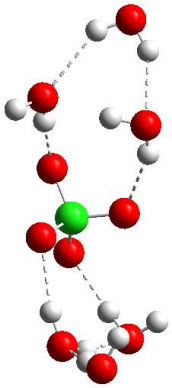

sm5

3.7 kcal/mol

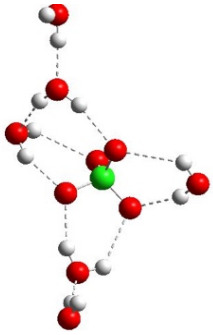

sm6

6.0 kcal/mol

Figure 6. Low-lying energy structural motifs and relative energies (DFTB3/3OB) of $ClO_4^-(H_2O)_6$

The structures show the resulting interplay between ion-water and water-water interactions. Interestingly, structural motifs 1-4 share structural similarity, with perchlorate pushed away from a network of clustered water molecules. In structural motifs 5 and 6, water molecules wrap around perchlorate and this breaks the water-water network, with significant energetic penalty.

2.3.3. Simulation of Larger $ClO_x^-(H_2O)_n$ [x = 1-4; n = 32, 64] Clusters

Results of REMD simulations of oxychloride anion-water clusters are discussed in this section. It is important to note that with 50 K increment between replicas in the simulation windows, the resulting exchange probability between two is less than 1.

Analysis of the structures of water clusters containing oxychlorides is first performed to gain an understanding of the effects of oxychlorides on the structure of water clusters, followed by that of dynamical features of the clusters from the calculated probability distributions of the distance between the oxychlorides and the cluster centre of mass.

Selected structures of $ClO_{1\text{-}4}^-(H_2O)_n$ clusters obtained from REMD simulations for n = 32 and 64 are shown in Figure 6. The major intermolecular interactions in the clusters occur between the O of oxychlorides and H of water molecules or O and H of water molecules as seen in the interatomic water-water interactions.

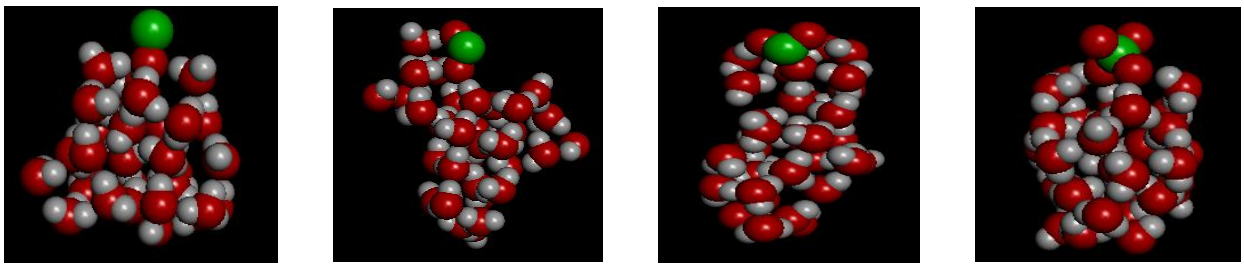

(a) $ClO^-(H_2O)_{32}$ $ClO_2^-(H_2O)_{32}$ $ClO_3^-(H_2O)_{32}$ $ClO_4^-(H_2O)_{32}$

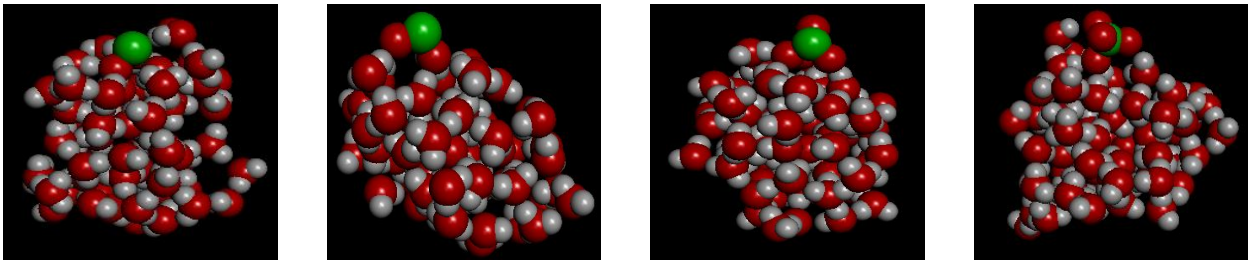

(b) $ClO^-(H_2O)_{64}$ $ClO_2^-(H_2O)_{64}$ $ClO_3^-(H_2O)_{64}$ $ClO_4^-(H_2O)_{64}$

Figure 7. Typical oxyhalide-water cluster conformations sampled by DFTB3/REMD simulations at 200 K

The effect of water network H-bonding cooperativity is seen to be dominant in the ion-water clusters and is due to the strong water-water interactions that drive the ions to the cluster surface. For the hypochlorite-containing clusters, the Cl atom is seen to protrude from the bulk cluster. This observed surface hydration is characteristic of all the oxychloride ions and the extent can be rationalized by analysing the probability distributions.

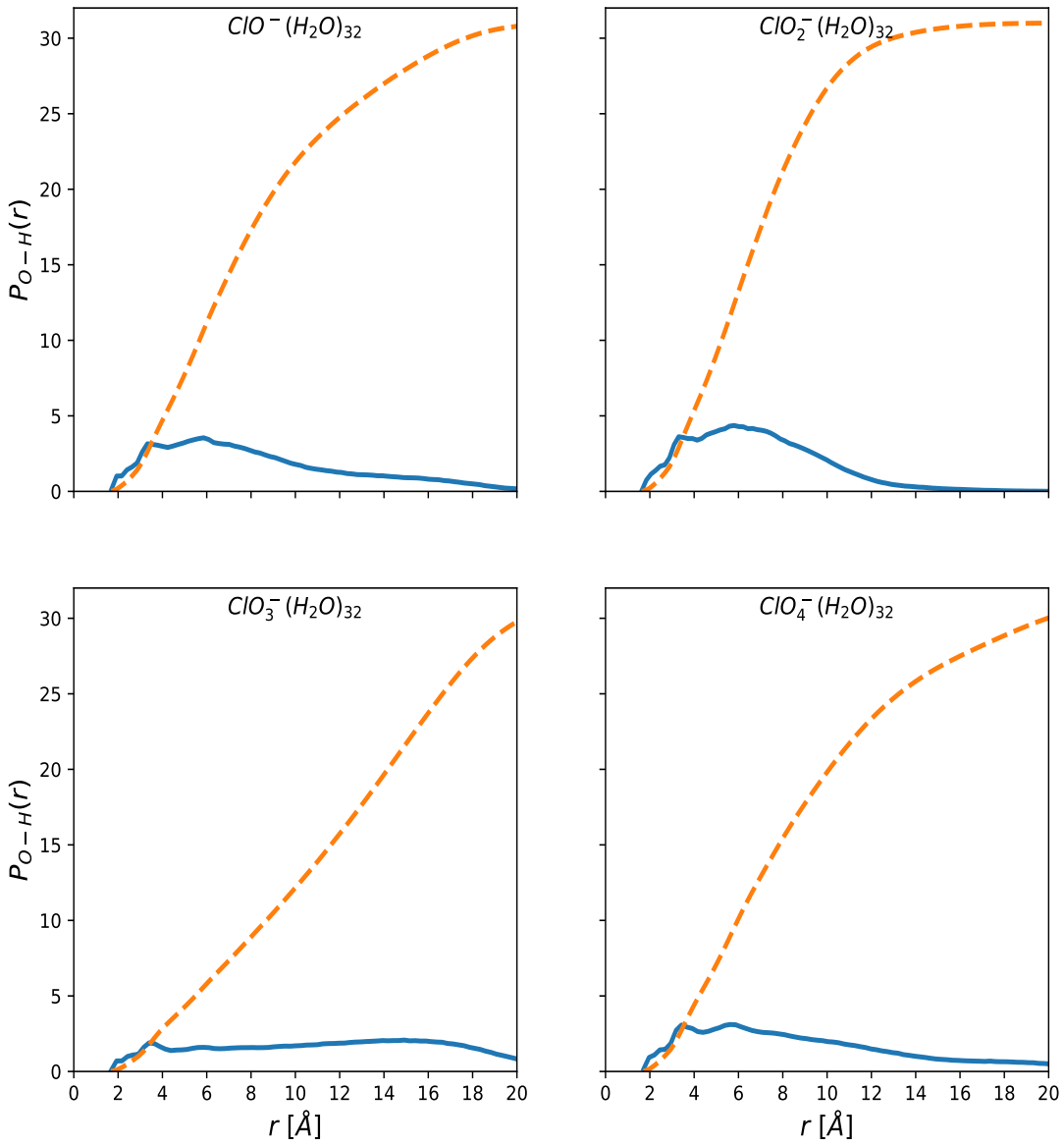

Figure 8. Structural properties of $ClO_{1\text{-}4}^-(H_2O)_{32}$ obtained from REMD-DFTB3 simulations at 200 K. Solid curves are radial probability distribution functions P(r), while dashed curves are the distance-dependent coordination number Ncoord(r) i.e., the integral of P(r)

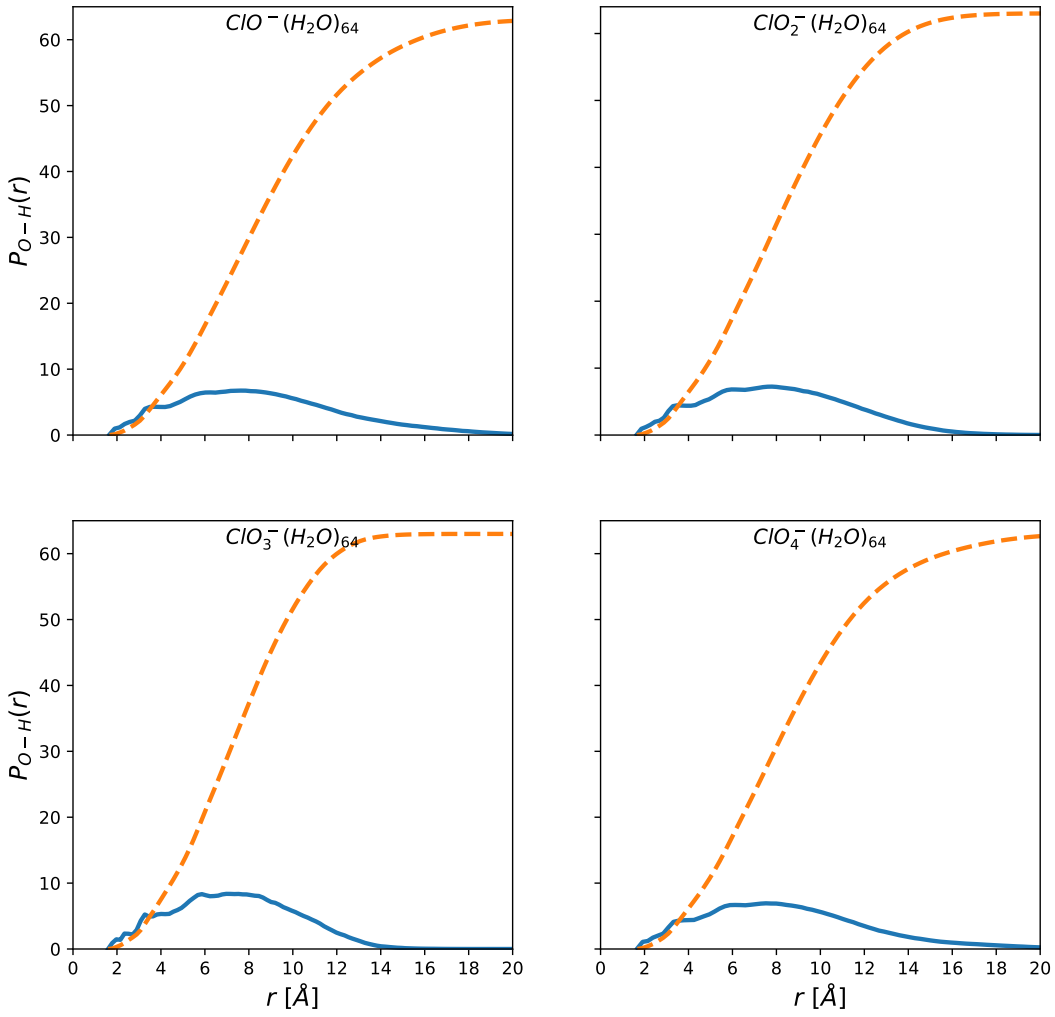

Figure 9. Structural properties of $ClO_{1\text{-}4}^-(H_2O)_{64}$ obtained from REMD-DFTB3 simulations at 200 K. Solid curves are radial probability distribution functions P(r), while dashed curves are the distance-dependent coordination number Ncoord(r), i.e., the integral of P(r)

Figures 8 and 9 show the radial intermolecular O-H probability distributions for $ClO_{1\text{-}4}^-(H_2O)_n$ clusters with n = 32 and 64. The ion-water intermolecular O-H probability distributions in Figure 8 differ from those of liquid water[63] in that they lack two distinct peaks, as seen for bulk water.

The intermolecular O-H distributions have a long tail, which is typical of a structureless solvent. The same effect is also evident for n=64 (Figure 9).

Figure 10 shows the spatial probability distributions of the oxychloride with respect to the water cluster center of mass for clusters containing 32 and 64 water molecules.

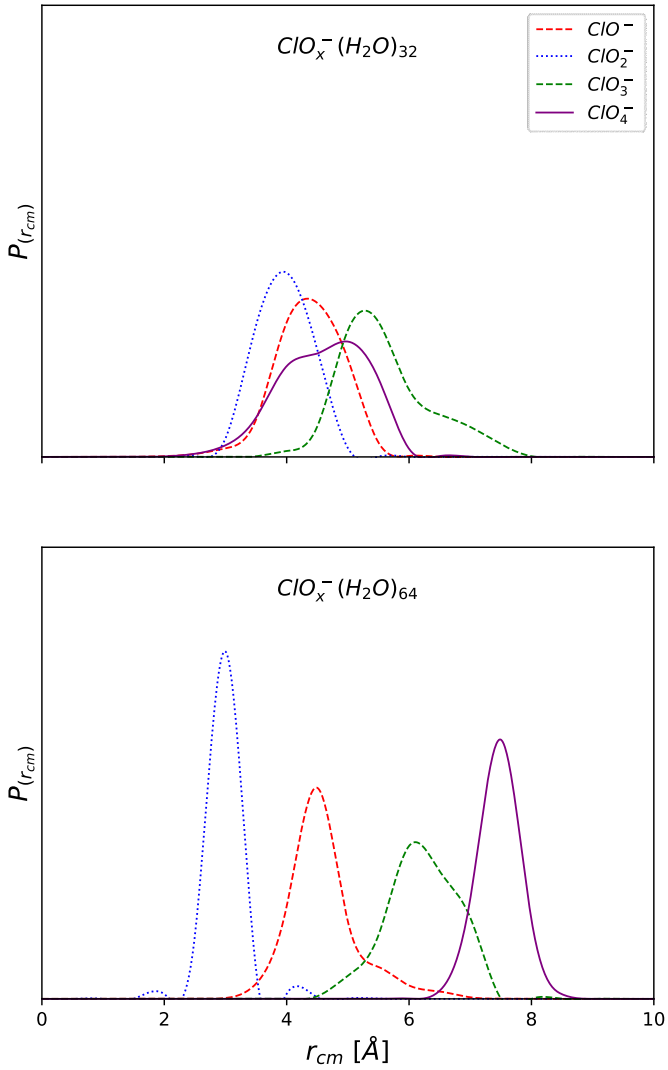

Figure 10. Probability distributions of the scaled ion-solvent center of mass distance r_{cm} in clusters of (a) $ClO_{1\text{-}4}^-(H_2O)_{32}$ (b) $ClO_{1\text{-}4}^-(H_2O)_{64}$ at 200K

Inspection of Figure 10 shows that for cluster size 32, the position of the oxychloride ions fluctuates at about the same distance from the cluster center of mass and they are located at the cluster surface. Interestingly, when the system size is doubled, chlorate and perchlorate show a higher preference for surface solvation than hypochlorite and chlorite ions (shift towards large distances from the water cluster center of mass).

2.4. Conclusion

The structural and energetic properties of water clusters containing ClO_x^- ions were explored. Results of ClO_x^- $(H_2O)_{1-4}$ cluster structural and energetic properties show that DFTB3 reproduces high level quantum chemistry data. For these small cluster sizes, the ion-water stepwise binding energies decrease as a function of cluster size. The influence of H-bond cooperativity in the structural stability of the small ion-water clusters was established.

The hydration of oxychloride was investigated by REMD simulations whereby the interatomic interactions were described by DFTB3. High temperature between two replicas reduced the probability of periodic swapping.

The results of the simulations show that ClO_x^- ions exhibit interfacial behaviour. The ions behave slightly similarly in clusters of 32 water molecules showing the tendency for partial surface hydration. When the system size is doubled, the surface affinity of the higher oxychloride ions (chlorate and the perchlorate) significantly surpasses those of hypochlorite and chlorite. This solvation preference may have consequences for the atmospheric chemistry of oxychlorides since it exposes the ions to reactions at the cluster surface.

Chapter 3

Microsolvation of Nitrogen Oxide Anions: Structural and Energetic Properties

3.1. Introduction

Studies have shown that the chemistry of ions in aqueous aerosols can be strongly influenced by their position, whether in the bulk or at the surface of aerosols.[64] Several experimental and theoretical studies have been carried out on the solvation and behavior of aqueous nitrogen oxide anions.[16,65–67] Over the years, scientists have debated whether a variety of ions, particularly nitrate, prefer to sit at the surface or dwell inside aqueous solutions.[16,68]

Aqueous NO_2^- and NO_3^- ions are of special interest because of their unique biological and physicochemical properties.[69–74] The NO_2^- ion also plays important roles in many atmospheric processes such as the nitrogen cycle. The NO_2^- ion possesses an ambidentate coordination via its lone pair of electrons on both oxygen and nitrogen sites. The NO_3^- ion is one of the most prevalent ions in the atmosphere, along with sulphate, bisulfate, and chloride; it can be found in both polluted and remote troposphere aerosols, and it plays a key role in various atmospheric chemical processes.[75]

Hydration of NO_x^- is important, among other factors, because there are relatively large concentrations of water in the atmosphere. Hence, studying this process will help to understand the molecular level anion–solvent and solvent–solvent interactions in aqueous phase. The first MD

simulation analysis of nitrate using a polarizable force field reported their behavior at the air-solution interface.[16,68] It was discovered that nitrate exhibits a preference for adsorbing at the air-water interface. More extensive force field based simulations of nitrate at extended bulk solution-air interfaces have consistently predicted that, while the nitrate ion is capable of visiting the interface, its concentration in the interfacial region is substantially depleted relative to the bulk solution, contrary to the original suggestion of pronounced interfacial propensity.[17,76,77]

Theoretically, the accurate description of intermolecular interactions as well as sampling of the available phase space are both demanding for a quantitative analysis of ion solvation in water clusters. *Ab initio* MD simulations have been well documented for the accurate description of intermolecular ion-solvent analysis.[65,78–82] However, a major caveat in *ab initio* MD simulations is the exponential rise in the demand for computational resources as the size of the system under study increases.

This work implements the third order expansion of the Density-Functional Tight-Binding (DFTB3) model to describe intermolecular interactions in ion-water clusters. The DFTB model allows for a thorough electronic description while limiting empiricism, with key parameters derived from traditional DFT. The usefulness of DFTB has become widely accepted with the inclusion of self-consistent charges (SCC-DFTB, also sometimes referred to as DFTB2)[37] and third-order correction terms (DFTB3).[83]

The phase space sampling is enhanced by implementing the replica exchange molecular dynamics (REMD) simulation technique.

3.2. Computational Details

This chapter follows the same computational procedures as the previous chapter.

3.3. Results and Discussion

3.3.1. Structural Properties and Bonding Topology of NO_x^- (H_2O) Binary Clusters

The optimized geometries of $NO_x^-(H_2O)$ binary clusters as shown in Figure 8 illustrate planar structures of nitrite and nitrate ions interacting via two electron-rich O atoms of the ions with two H atoms of water molecule.

Figure 11. Optimized structures of NO_x^- (H_2O) binary clusters at MP2/aug-cc-pVTZ level

The geometric properties calculated from two levels of theory are shown in Table 3. The calculated O..H-O bond angles obtained from DFTB3 model deviate from MP2 results by about 1-3° while the O..H-O hydrogen bond distance obtained from DFTB3 slightly underestimate results obtained from MP2.

Table 3. Selected geometric properties of binary clusters

Clusters	MP2/aug-cc-pVTZ	DFTB3/3OB
Bond angles (°)		
NO_2^- (H_2O)	142.8	140.1
NO_3^- (H_2O)	142.6	144.0
Δ		**2.1**
Bond Length (r) (Å)		
NO_2^- (H_2O)	2.00	1.79
NO_3^- (H_2O)	2.13	1.92
Δ		**0.7**

Δ is the absolute mean deviation of the DFTB data from MP2/aug-cc-pVTZ data.

The AIM plots of the binary clusters showing the bond critical points and electron density paths are obtained. The interaction was investigated through the molecular graph (Figure 12). The Laplacian obtained from the analysis of the bond critical points confirm a non-covalent type of interaction.

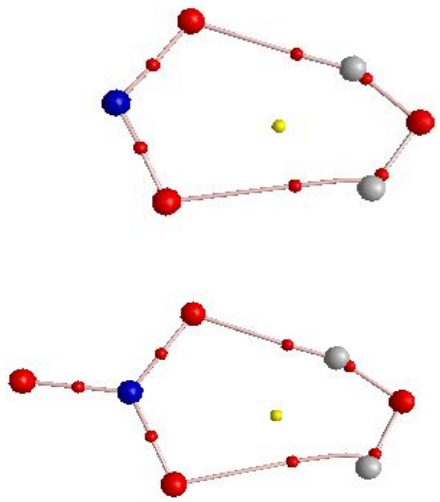

ρBCP (r) = 0.218 e/Å^3

$\nabla^2\rho(r)$ = 2.05 e/Å^5

ρBCP (r) = 0.227 e/Å^3

$\nabla^2\rho(r)$ = 2.15 e/Å^5

Figure 12. Molecular graphs of NO_x^- (H_2O) binary clusters (a) NO_2^- (H_2O) (b) NO_3^- (H_2O) showing the electron densities and Laplacian values at selected bond critical point (BCP)

In accordance with Popelier's criteria, the electron density ρBCP at the BCPs are in the range 0.001-0.270 e/Å^3 for a hydrogen bond.[84,85] The electron densities at the BCPs for NO_2^- (H_2O) and NO_3^- (H_2O) are 0.218 and 0.227 e/Å^3 respectively. The positive sign of the Laplacian $\nabla^2\rho(r)$ obtained at the selected BCPs of the dimers (see Figure 12) also confirm the non-covalent nature of the dimers.

3.3.2. Binding Strength

The stepwise binding energies of nitrogen anion-water clusters obtained when an additional water molecule interacts with the cluster is calculated. It follows from Table 4 that the stepwise binding energies decrease (about 1-3 kcal/mol) as a function of cluster size and are lower for $NO_3^-(H_2O)_n$. It is not surprising to know that the ions tend to interact weakly with water molecules as the cluster size increases. It is also possible to derive a comparable trend from the results of CCSD(t)//MP2 and DFTB3 models that provide a basic understanding for nitrogen oxide anion-water interactions.

In addition, this provides information on the assessment of the performance of DFTB3/3OB model in producing energetic properties that can be compared with high-level quantum chemistry calculation results.

Table 4. Stepwise binding energies of $NO_2^-(H_2O)_{1-3}$ and $NO_3^-(H_2O)_{1-3}$ clusters

	$NO_2^-(H_2O)_n$		$NO_3^-(H_2O)_n$	
n	CCSD (T)	DFTB3	CCSD (T)	DFTB3
1	13.7	15.8	11.9	14.8
2	11.4	13.3	10.7	13.8
3	9.8	12.3	9.6	12.6
Δ		2.2		3.0

All values are in kcal/mol. Results from CCSD(T)//MP2/aug-cc-pVTZ and DFTB3/OB calculations. Δ is the absolute mean deviation of the DFTB data from MP2/aug-cc-pVTZ data

Figure 13 shows the optimized structures and relative energies of selected low-lying energy conformations of $NO_x^-(H_2O)_2$ and $NO_x^-(H_2O)_3$ clusters. Planar and non-planar forms are observed in both $NO_2^-(H_2O)_2$ and $NO_3^-(H_2O)_2$. In clusters containing two water molecules, for instance, in the case of $NO_2^-(H_2O)_2$ (Figure 13a), the more stable planar structure indicates a free H atom available for interaction with a neighboring water molecule. Planar structure is also favoured in $NO_3^-(H_2O)_2$ and $NO_3^-(H_2O)_3$ clusters (Figures 13b and 13c), whereby each water molecule is directly coordinated to the nitrate O-atoms through the two H-atoms. It is also important to note that each oxygen atom in the NO_x^- forms a maximum of 2 hydrogen bonds with water.

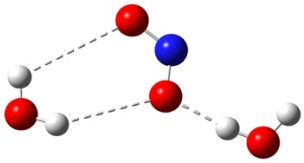

E = 0 kcal/mol

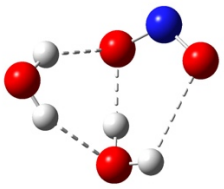

E = 0.9 kcal/mol

(a)

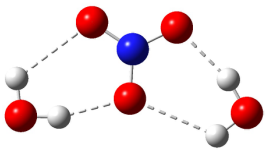

E = 0 kcal/mol

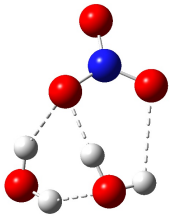

E = 1.3 kcal/mol

(b)

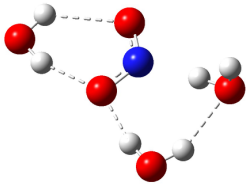

E = 0 kcal/mol

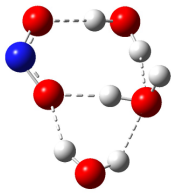

E = 0.8 kcal/mol

(c)

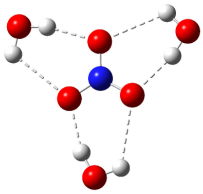

E = 0 kcal/mol

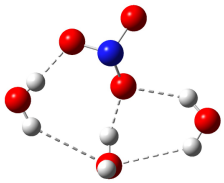

E = 1.5 kcal/mol

(d)

Figure 13. Optimized structures (MP2/aug-cc-pVTZ) and relative energies of low-lying energy conformations of $NO_x^-(H_2O)_2$ and $NO_x^-(H_2O)_3$ clusters

3.3.3. Simulation of Clusters

Time evolution structures of $NO_x^-(H_2O)_n$ (x = 2 and 3 ; n = 32 and 64) are generated from the enhanced sampling of nitrogen oxide anion-water clusters by REMD simulations for 120ps.

Analysis of the structures of water clusters containing nitrogen oxide anions are first examined to provide fundamental insights into the interplay between water molecules and NO_x^- in the clusters, followed by the dynamical features of the clusters by considering the probability distributions of the distance between NO_x^- ion and the cluster centre of mass.

Cluster Structures and Ion Hydration in NO_x^- $(H_2O)_n$; n = 32 and 64

Figure 14 shows representative structures of NO_x^- $(H_2O)_n$ at 200 K for cluster sizes n = 32 and 64 observed through simulation.

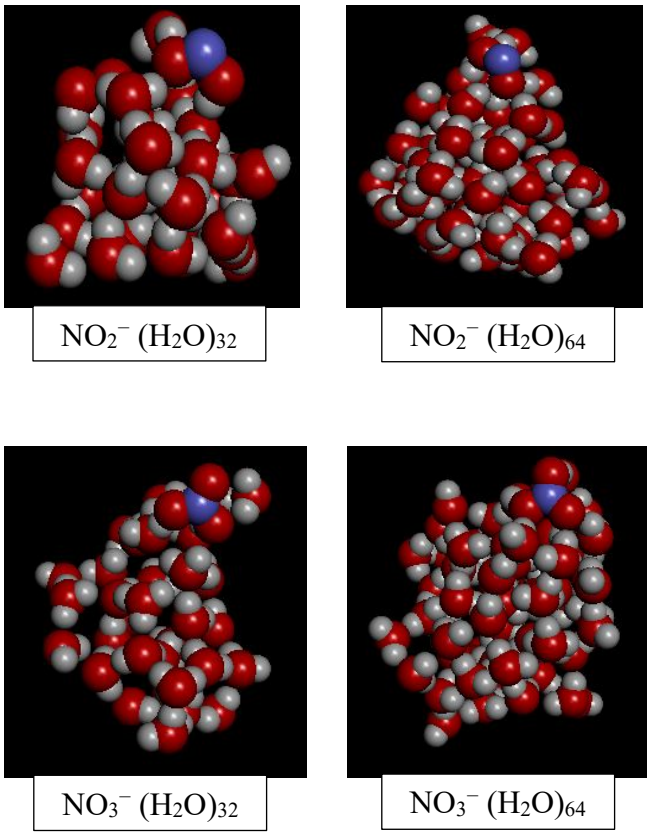

Figure 14. Snapshots of typical NO_x^- $(H_2O)_n$ [n=32 and 64] clusters conformations during DFTB3/REMD simulations at 200 K

According to Figure 14, the NO_x^- ions reside at the surface of both cluster sizes. It can be seen that the solvent molecules prefer to interact with neighbouring solvent molecules, resulting

in a network of water-water H-bonding. This effect initiates the repulsion of the ion towards the cluster surface.

Figures 15 and 16 show the radial intermolecular O-H probability distributions for $NO_x^-(H_2O)_{32}$ and $NO_x^-(H_2O)_{64}$ clusters. The absence of distinct peaks and presence of a long tail in the ion-water intermolecular O-H probability distributions are common features in structureless solvents. This may be as a result of the weak water cluster perturbation by the polyatomic ions, a phenomenon typical of chaotropic solutes.

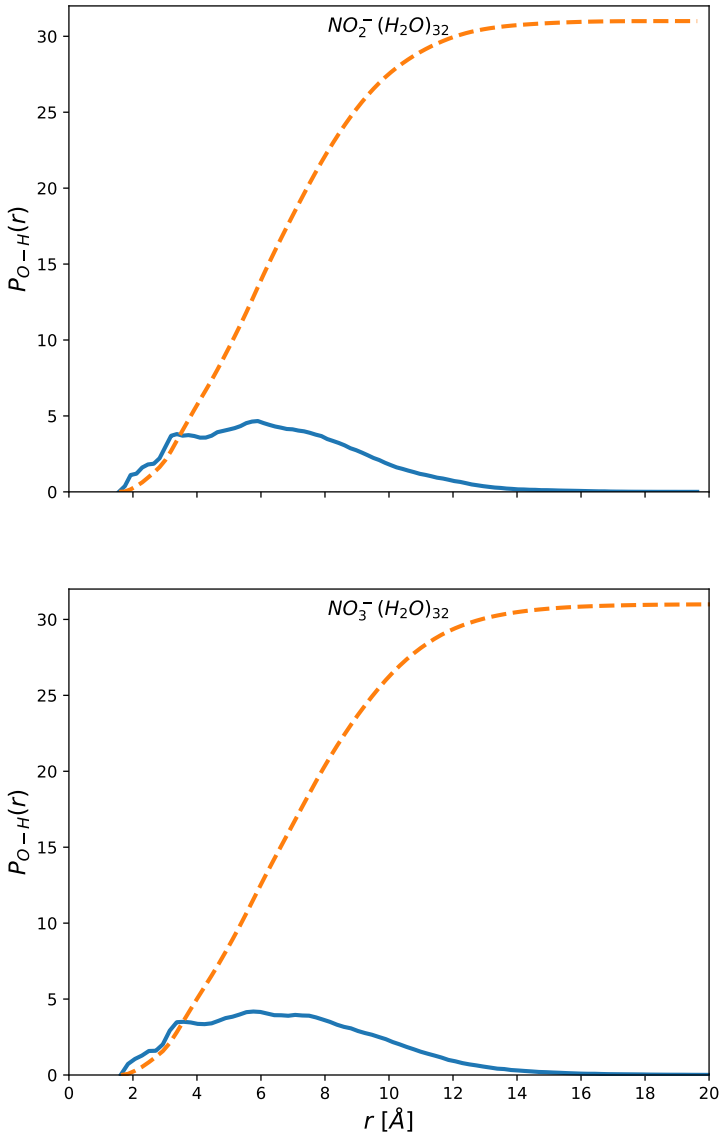

Figure 15. Structural properties of $NO_2^-(H_2O)_{32}$ and $NO_3^-(H_2O)_{32}$ obtained from REMD-DFTB3 simulations at 200 K. Solid curves are radial probability distribution functions P(r), while dashed curves are the distance-dependent coordination number Ncoord(r), i.e., the integral of P(r)

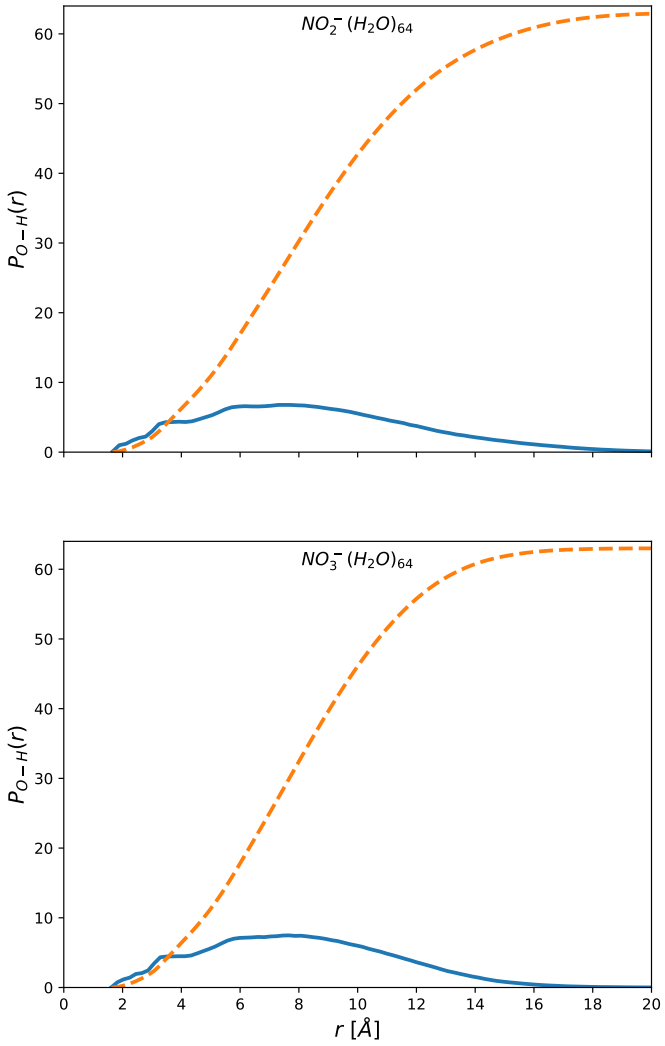

Figure 16. Structural properties of $NO_2^-(H_2O)_{64}$ and $NO_3^-(H_2O)_{32}$ obtained from REMD-DFTB3 simulations at 200 K. Solid curves are radial probability distribution functions P(r), while dashed curves are the distance-dependent coordination number Ncoord(r), i.e., the integral of P(r)

In order to provide further insight into the dynamical feature of the ion-water clusters, the probability distribution of the ions from the cluster center of mass was obtained from the PMF of the systems.

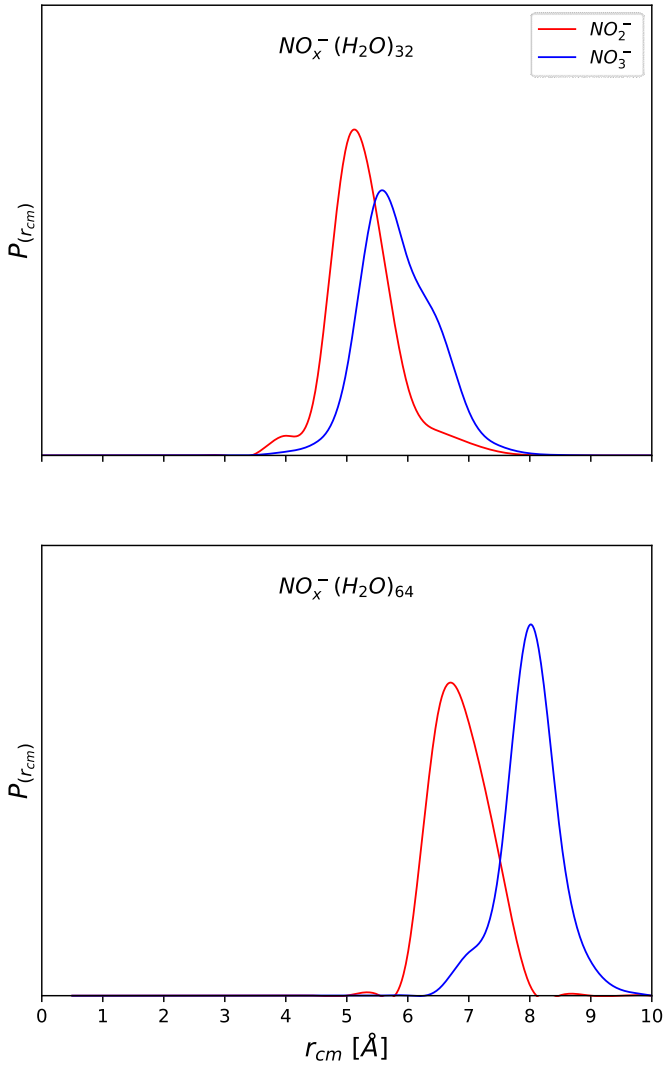

Figure 17. Probability distributions of the scaled ion-solvent center of mass distance r_{cm} in clusters of $NO_x^-(H_2O)_{32}$ and $NO_x^-(H_2O)_{64}$

The spatial probability distributions of NO_x^- with respect to the scaled water cluster center of mass for clusters containing 32 and 64 water molecules are shown in Figure 17. In the water cluster size containing 32 water molecules, nitrite and nitrate ions fluctuate about the same distance from the

cluster center of mass. Interestingly, when the system size is doubled, nitrate ion shows a higher preference (peak at 8 Å) for surface solvation than nitrite (peak around 6.5 Å). This feature is particularly significant in the atmospheric chemistry of these ions.

3.4. Conclusion

The solvation of NO_x^- ions was investigated using MD simulations. The performance of the DFTB3 in predicting the structural and energetic properties of water clusters containing NO_x^- was first validated by comparing the results against those of high-level quantum chemistry calculations. From the energetic properties point of view, DFTB3 reproduces the same trends as those obtained from high level calculations while the deviation of the geometric properties is within acceptable range.

Interestingly, results from the DFTB3/3OB model are obtained at a fraction of the computational cost of high-level quantum calculation results and this gives a good compromise between accuracy and computational cost. For small $NO_x^-(H_{2x}O)_n$ [$x = 2$ or 3; $n \leq 3$] clusters, stepwise ion-water binding energies decrease as a function of cluster size; the most stable conformations reflect a stronger preference for water molecules to interact with each other rather than with the ion.

Furthermore, the hydration of NO_x^- investigated by REMD simulations confirms the interfacial behaviour of NO_x^- ions; nitrite and nitrate ions behave similarly in clusters with 32 water molecules, exhibiting a preference for partial hydration at the cluster surface. On doubling the system size, the surface affinity of nitrate is increased. The NO_x^- ions are found to form a maximum of 2 hydrogen bonds with water molecules through the ion O and water H atoms. This is consistent with the outcome of recent *ab initio* studies.[65]

Chapter 4

Conclusion and Outlook

4.1. Summary and Conclusion

In this thesis, MD simulations were used to study the solvation preferences of oxychlorides and nitrogen oxide anions in water clusters. In order to improve conformational sampling of the clusters, a parallel tempering approach known as REMD was adopted. The DFTB3 model was first validated against high-level quantum chemistry calculations of geometric and energetic properties, and thereafter employed to describe intermolecular interactions.

The high temperature difference between two consecutive replicas reduced the probability of periodic swapping according to the Metropolis-Hastings criterion.

In chapter 2, properties of water clusters containing oxychlorides were considered. The calculated stepwise binding energies of small $ClO_x^-(H_2O)_n$ clusters ($n \leq 4$) decrease as a function of cluster size and increasing chlorine oxidation number. The results revealed that as the number of water molecules in the cluster increases, the effect of H-bond cooperativity in the structural stability of the ion-water clusters becomes more apparent. DFTB3 showed promising ability to predict lower energy conformers within smaller clusters based on preliminary calculations. To characterize the extent of hydration, potential of mean force calculation was performed on the clusters. The simulation results demonstrated that ClO_x^- ions exhibit interfacial behaviour in water

clusters containing 32 water molecules. On doubling the system size the phenomenon becomes more pronounced for ClO_3^- and ClO_4^-.

In chapter 3, properties of water clusters containing nitrite and nitrate ions were considered. For small cluster sizes, the stepwise binding energies of nitrate are weaker than those of nitrites. The thermodynamical properties of the water clusters up to 64 show that NO_2^- and NO_3^- both have high propensity for surface hydration. These simulations showed that nitrate has a stronger preference for surface hydration than nitrite, although both ions exhibit weak interactions with water molecules. The observed weak ion-water interaction conforms with results obtained from small clusters in preliminary calculations. This feature may influence the chemistry of these ions as they will be readily available for reactions with atmospheric particles.

4.2. Outlook

The research lays the groundwork for the development of advanced methods for simulating water clusters containing polyatomic ions. There is a need to continuously improve on simulation methodologies, not only to make the techniques less cumbersome but also to ensure a more rigorous approach for simulation. The simulation methodology of water clusters could be improved in the future by rigorously comparing the output of various MD simulation algorithms such as rigid-body quaternions[86] to those of the present simulations using RATTLE,[87] as such information is still lacking in the literature. Quaternion-based rigid body algorithm is well suited for representing the rotation of rigid bodies while RATTLE algorithm is implemented in molecular models with internal constraint.

The thermodynamics of ion hydration in clusters are of importance towards understanding the solvation process, as spatial probability distributions of ions within the water clusters can for example be obtained rigorously from PMFs, i.e. free energy changes along a selected coordinate,

as was demonstrated in chapters 2 and 3. Standard equilibrium methods for free energy calculations are computationally intensive and much effort has been devoted towards the development of alternate free energy calculation approaches. The application of nonequilibrium techniques in calculating equilibrium properties can be relevant with respect to this direction.

Phase transition in clusters may have great implications in the environmental influence of atmospheric clusters and the influence of ions on this phenomenon may vary from one ion to the other. The phase behavior observed in water clusters can be different from that in the bulk, with changes in the melting temperature that may depend on cluster size. Most research works in that area have been limited to pure water clusters. Investigating finite-temperature properties of ion-water clusters may provide valuable information towards understanding the specific role(s) of seeding agents (presence and positional effects) in cluster phase transitions.

This research focuses on a single solvent system, water. The solvation of ions in mixed solvent systems may yield different results and provide answers to existing questions on phase separation. The development of a methodology for simulating clusters containing molecular species and mixed solvent based on the present work will be interesting to consider as part of future work. The hydration of oxychlorides is certainly important to atmospheric chemistry, but extending this research to include a broad variety of oxyanions containing bromine and iodine, such as $BrO_{1\text{-}4}^{-}$ and $IO_{1\text{-}4}^{-}$ might yield more valuable information to answer certain environmental questions such as the composition of aerosol mass. Furthermore, based on the reliability of the DFTB3 model demonstrated in this research for the selected polyatomic ions, a possible direction to extend this research work is to investigate cluster hydration focused on acid dissociation of $HClO_4$ and HNO_3. Most research works in that area have been limited to hydrated bisulphate

clusters. An interesting question to consider regarding the acid dissociation is solvation of the proton.

In order to properly model the three-dimensional hydrogen bonding network in water, future work may focus on environmentally relevant ions solvated in larger clusters of size up to 128 and 256 water molecules. Finally, the high temperature difference between two adjacent replicas selected here significantly reduced the probability of periodic swapping according to the Metropolis-Hastings criterion in the course of the REMD simulations, which warrants further investigation of the performance of conformational sampling with respect to the temperature distributions of the REMD simulations.

References

1. Sato H. A modern solvation theory: quantum chemistry and statistical chemistry. *Phys Chem Chem Phys*. 2013;15(20):7450.

2. Chang TM, Dang LX. Recent Advances in Molecular Simulations of Ion Solvation at Liquid Interfaces. *Chem Rev*. 2006;106(4):1305-1322.

3. Frutos-Puerto S, Aguilar MA, Fdez. Galván I. Theoretical Study of the Preferential Solvation Effect on the Solvatochromic Shifts of *para* -Nitroaniline. *J Phys Chem B*. 2013;117(8):2466-2474.

4. Jordanides XJ, Lang MJ, Song X, Fleming GR. Solvation Dynamics in Protein Environments Studied by Photon Echo Spectroscopy. *J Phys Chem B*. 1999;103(37):7995-8005.

5. Lábas A, Bakó I, Oláh J. Hydration sphere structure of proteins: A theoretical study. *Journal of Molecular Liquids*. 2017;238:462-469.

6. Gaston N. Cluster melting: New, Limiting, and Liminal Phenomena. *Advances in Physics: X*. 2018;3(1):1401487.

7. Kane RS, Deschatelets P, Whitesides GM. Kosmotropes Form the Basis of Protein-Resistant Surfaces. *Langmuir*. 2003;19(6):2388-2391.

8. Yamniuk AP, Ditto N, Patel M, et al. Application of a Kosmotrope-Based Solubility Assay to Multiple Protein Therapeutic Classes Indicates Broad Use as a High-Throughput Screen for Protein Therapeutic Aggregation Propensity. *Journal of Pharmaceutical Sciences*. 2013;102(8):2424-2439.

9. Ohtaki Hitoshi, Radnai Tamas. Structure and dynamics of hydrated ions. *Chem Rev*. 1993;93(3):1157-1204.

10. Mähler J, Persson I. A Study of the Hydration of the Alkali Metal Ions in Aqueous Solution. *Inorg Chem*. 2012;51(1):425-438.

11. Zhan CG, Dixon DA. Hydration of the Fluoride Anion: Structures and Absolute Hydration Free Energy from First-Principles Electronic Structure Calculations. *J Phys Chem A*. 2004;108(11):2020-2029.

12. Science G. Mixed Chloride Aerosols and their Atmospheric Implications: A Review. *Aerosol Air Qual Res*. 2017;17(4):878-887.

13. Siddiqui MS. Chlorine-ozone interactions: Formation of chlorate. *Water Research*. 1996;30(9):2160-2170.

14. Rao B, Anderson TA, Redder A, Jackson WA. Perchlorate Formation by Ozone Oxidation of Aqueous Chlorine/Oxy-Chlorine Species: Role of Cl_x O_y Radicals. *Environ Sci Technol*. 2010;44(8):2961-2967.

15. Handa D, Okada K, Nakajima H, Arakaki T. Perchlorate Ion in Aerosols Collected at Cape Hedo, Okinawa, Japan. *Earozoru Kenkyu*. 2010;25(3):269-273.

16. Salvador P, Curtis JE, Tobias DJ, Jungwirth P. Polarizability of the nitrate anion and its solvation at the air/water interface. *Phys Chem Chem Phys*. 2003;5(17):3752-3757.

17. Dang LX, Chang TM, Roeselova M, Garrett BC, Tobias DJ. On NO_3^-–H_2O interactions in aqueous solutions and at interfaces. *J Chem Phys*. 2006;124(6):066101.

18. Okuwaki K, Mochizuki Y, Doi H, Kawada S, Ozawa T, Yasuoka K. Theoretical analyses on water cluster structures in polymer electrolyte membrane by using dissipative particle dynamics simulations with fragment molecular orbital based effective parameters. *RSC Advances*. 2018;8(60):34582-34595.

19. Brodskaya EN, Rusanov AI. Molecular-dynamics simulation of water clusters with ions. *Molecular physics*. 1990;71(3):567-585.

20. Martys NS, Mountain RD. Velocity Verlet algorithm for dissipative-particle-dynamics-based models of suspensions. *Phys Rev E*. 1999;59(3):3733-3736.

21. Evans DJ, Holian BL. The Nose–Hoover thermostat. *The Journal of Chemical Physics*. 1985;83(8):4069-4074.

22. Earl DJ, Deem MW. Parallel tempering: Theory, applications, and new perspectives. *Phys Chem Chem Phys*. 2005;7(23):3910-3916.

23. Kollman Peter. Free energy calculations: Applications to chemical and biochemical phenomena. *Chem Rev*. 1993;93(7):2395-2417.

24. Hansen N, van Gunsteren WF. Practical Aspects of Free-Energy Calculations: A Review. *J Chem Theory Comput*. 2014;10(7):2632-2647.

25. Torrie GM, Valleau JP. Nonphysical sampling distributions in Monte Carlo free-energy estimation: Umbrella sampling. *Journal of Computational Physics*. 1977;23(2):187-199.

26. Hummer G. Fast-growth thermodynamic integration: Error and efficiency analysis. *The Journal of Chemical Physics*. 2001;114(17):7330-7337.

27. Jorgensen WL, Thomas LL. Perspective on Free-Energy Perturbation Calculations for Chemical Equilibria. *J Chem Theory Comput*. 2008;4(6):869-876.

28. Kumar S, Rosenberg JM, Bouzida D, Swendsen RH, Kollman PA. The weighted histogram analysis method for free-energy calculations on biomolecules. I. The method. Journal of computational chemistry. 1992;13(8):1011-21

29. Řezáč J, Šimová L, Hobza P. CCSD[T] Describes Noncovalent Interactions Better than the CCSD(T), CCSD(TQ), and CCSDT Methods. *J Chem Theory Comput*. 2013;9(1):364-369.

30. Feyereisen M, Fitzgerald G, Komornicki A. Use of approximate integrals in ab initio theory. An application in MP2 energy calculations. *Chemical Physics Letters*. 1993;208(5-6):359-363.

31. Baboul AG, Curtiss LA, Redfern PC, Raghavachari K. Gaussian-3 theory using density functional geometries and zero-point energies. *The Journal of Chemical Physics*. 1999;110(16):7650-7657.

32. Gross EKU, Ullrich CA, Gossmann UJ. In Density Functional Theory; Gross, EKU; Dreizler, RM, Eds. In: *NATO Advanced Study Institute Series B: Physics*. 1995:149-171.

33. Seminario JM. *Recent Developments and Applications of Modern Density Functional Theory*. Elsevier; 1996.

34. Parr RG. Density Functional Theory. *Annu Rev Phys Chem*. 1983;34(1):631-656.

35. Hohenberg P, Kohn W. Inhomogeneous Electron Gas. *Phys Rev*. 1964;136(3B):B864-B871.

36. Frauenheim T, Seifert G, Elstner M, et al. Atomistic simulations of complex materials: ground-state and excited-state properties. *J Phys: Condens Matter*. 2002;14(11):3015-3047.

37. Elstner M, Porezag D, Jungnickel G, et al. Self-consistent-charge density-functional tight-binding method for simulations of complex materials properties. *Phys Rev B*. 1998;58(11):7260-7268.

38. Foulkes WMC, Haydock R. Tight-binding models and density-functional theory. *Phys Rev B*. 1989;39(17):12520-12536.

39. A Self-Consistent Charge Density-Functional Based Tight-Binding Method for Predictive Materials Simulations in Physics, Chemistry and Biology - Frauenheim - 2000 - physica status solidi (b)

40. Jahangiri S, Cai L, Peslherbe GH. Performance of density-functional tight-binding models in describing hydrogen-bonded anionic-water clusters. *J Comput Chem*. 2014;35(23):1707-1715.

41. Gaus M, Cui Q, Elstner M. DFTB3: extension of the self-consistent-charge density-functional tight-binding method (SCC-DFTB). Journal of chemical theory and computation. 2011;7(4):931-48.

42. Gokel GW. A Review of "Phase-transfer catalysis fundamentals, applications, and industrial perspectives. *Supramolecular Chemistry*. 1995;5(3):237-237.

43. Okur HI, Hladílková J, Rembert KB, et al. Beyond the Hofmeister Series: Ion-Specific Effects on Proteins and Their Biological Functions. *J Phys Chem B*. 2017;121(9):1997-2014.

44. Tadeo X, Pons M, Millet O. Influence of the Hofmeister Anions on Protein Stability As Studied by Thermal Denaturation and Chemical Shift Perturbation. *Biochemistry*. 2007;46(3):917-923.

45. Eisele FL, Lovejoy ER, Kosciuch E, et al. Negative atmospheric ions and their potential role in ion-induced nucleation. *Journal of Geophysical Research: Atmospheres*. 2006;111(D4).

46. Cabarcos OM, Weinheimer CJ, Lisy JM, Xantheas SS. Microscopic hydration of the fluoride anion. *The Journal of Chemical Physics*. 1999;110(1):5-8.

47. Trumm M, Martínez YOG, Réal F, Masella M, Vallet V, Schimmelpfennig B. Modeling the hydration of mono-atomic anions from the gas phase to the bulk phase: The case of the halide ions F^-, Cl^- and Br^-. *The Journal of Chemical Physics*. 2012;136(4):044509.

48. Yoo S, Lei YA, Zeng XC. Effect of polarizability of halide anions on the ionic solvation in water clusters. *The Journal of Chemical Physics*. 2003;119(12):6083-6091.

49. Ohgushi T, Ishimaru K, Adachi Y. Movements and Hydration of Potassium Ion in K-A Zeolite. *J Phys Chem C*. 2009;113(6):2468-2474.

50. Falkowska L, Lewandowska A. Sulphates in particles of different sizes in the marine boundary layer over the Southern Baltic Sea. *Oceanologia*. 2004;46(2).

51. Johansson G. Structures of Complexes in Solution Derived from X-Ray Diffraction Measurements. In: *Advances in Inorganic Chemistry*. Vol 39. Elsevier; 1992:159-232.

52. Neilson GW. Diffraction studies of aqueous electrolyte solutions. *Pure and Applied Chemistry*. 1988;60(12):1797-1806.

53. Eklund L, Hofer TS, Persson I. Structure and water exchange dynamics of hydrated oxo halo ions in aqueous solution using QMCF MD simulation, large angle X-ray scattering and EXAFS. *Dalton Trans*. 2015;44(4):1816-1828.

54. Maekawa Y, Sasaoka K, Yamamoto T. Structure of water clusters on graphene: A classical molecular dynamics approach. *Jpn J Appl Phys*. 2018;57(3):035102.

55. Hofmann DWM, Kuleshova L, D'Aguanno B, et al. Investigation of Water Structure in Nafion Membranes by Infrared Spectroscopy and Molecular Dynamics Simulation. *J Phys Chem B*. 2009;113(3):632-639.

56. Møller Chr, Plesset MS. Note on an Approximation Treatment for Many-Electron Systems. *Phys Rev*. 1934;46(7):618-622.

57. Gaus M, Goez A, Elstner M. Parametrization and Benchmark of DFTB3 for Organic Molecules. *J Chem Theory Comput*. 2013;9(1):338-354.

58. Gelman-Constantin J, Carignano MA, Szleifer I, Marceca EJ, Corti HR. Structural transitions and dipole moment of water clusters $(H_2O)_{n=4–100}$. *The Journal of Chemical Physics*. 2010;133(2):024506.

59. Burnham CJ, Petersen MK, Day TJF, Iyengar SS, Voth GA. The properties of ion-water clusters. II. Solvation structures of Na^+, $Cl^–$, and H^+ clusters as a function of temperature. *The Journal of Chemical Physics*. 2006;124(2):024327.

60. Frisch MJ, Clemente FR. Gaussian 09, Rev. A. 01, MJ Frisch, GW Trucks, HB Schlegel, GE Scuseria, MA Robb, JR Cheeseman, G. *Scalmani, V Barone, B Mennucci, GA Petersson, H Nakatsuji, M Caricato, X Li, HP Hratchian, AF Izmaylov, J Bloino, G Zhe*. 2009;121:150-66

61. Aradi B, Hourahine B, Frauenheim T. DFTB+, a sparse matrix-based implementation of the DFTB method. The Journal of Physical Chemistry A. 2007 ;111(26):5678-84

62. Aim2000. *Journal of Computational Chemistry*. 2001;22(5):545-559.

63. Chialvo AA, Cummings PT. Engineering a simple polarizable model for the molecular simulation of water applicable over wide ranges of state conditions. *The Journal of Chemical Physics*. 1996;105(18):8274-8281.

64. Ruiz-Lopez MF, Francisco JS, Martins-Costa MTC, Anglada JM. Molecular reactions at aqueous interfaces. *Nat Rev Chem*. 2020;4(9):459-475.

65. Yadav S, Chandra A. Solvation Shell of the Nitrite Ion in Water: An Ab Initio Molecular Dynamics Study. *J Phys Chem B*. 2020;124(33):7194-7204.

66. Yadav S, Choudhary A, Chandra A. A First-Principles Molecular Dynamics Study of the Solvation Shell Structure, Vibrational Spectra, Polarity, and Dynamics around a Nitrate Ion in Aqueous Solution. *J Phys Chem B*. 2017;121(38):9032-9044.

67. Pruitt SR, Brorsen KR, Gordon MS. Ab initio investigation of the aqueous solvation of the nitrate ion. *Phys Chem Chem Phys*. 2015;17(40):27027-27034.

68. Brown MA, Winter B, Faubel M, Hemminger JC. Spatial Distribution of Nitrate and Nitrite Anions at the Liquid/Vapor Interface of Aqueous Solutions. *J Am Chem Soc*. 2009;131(24):8354-8355.

69. Jungwirth P, Winter B. Ions at Aqueous Interfaces: From Water Surface to Hydrated Proteins. *Annu Rev Phys Chem*. 2008;59(1):343-366.

70. Chameides WL, Stelson AW. Aqueous-phase chemical processes in deliquescent sea-salt aerosols: A mechanism that couples the atmospheric cycles of S and sea salt. *J Geophys Res*. 1992;97(D18):20565.

71. Angle KJ, Neal EE, Grassian VH. Enhanced Rates of Transition-Metal-Ion-Catalyzed Oxidation of S(IV) in Aqueous Aerosols: Insights into Sulfate Aerosol Formation in the Atmosphere. *Environ Sci Technol*. 2021;55(15):10291-10299.

72. Moustakas M. The Role of Metal Ions in Biology, Biochemistry and Medicine. *Materials (Basel)*. 2021;14(3):549.

73. Collins KD. Sticky ions in biological systems. *Proceedings of the National Academy of Sciences*. 1995;92(12):5553-5557.

74. Kunz W. Specific ion effects in colloidal and biological systems. *Current Opinion in Colloid & Interface Science*. 2010;15(1-2):34-39.

75. Gibson ER, Hudson PK, Grassian VH. Physicochemical properties of nitrate aerosols: implications for the atmosphere. *J Phys Chem A*. 2006;110(42):11785-11799.

76. Thomas JL, Roeselová M, Dang LX, Tobias DJ. Molecular Dynamics Simulations of the Solution−Air Interface of Aqueous Sodium Nitrate. *J Phys Chem A*. 2007;111(16):3091-3098.

77. Minofar B, Vácha R, Wahab A, Mahiuddin S, Kunz W, Jungwirth P. Propensity for the Air/Water Interface and Ion Pairing in Magnesium Acetate vs Magnesium Nitrate Solutions: Molecular Dynamics Simulations and Surface Tension Measurements. *J Phys Chem B*. 2006;110(32):15939-15944.

78. Leung K, Rempe SB. Ab Initio Molecular Dynamics Study of Formate Ion Hydration. *J Am Chem Soc*. 2004;126(1):344-351.

79. Marx D, Parrinello M. Ab initio path-integral molecular dynamics. *Z Physik B - Condensed Matter*. 1994;95(2):143-144.

80. Tuckerman M, Laasonen K, Sprik M, Parrinello M. Ab Initio Molecular Dynamics Simulation of the Solvation and Transport of H_3O^+ and OH^- Ions in Water. *J Phys Chem*. 1995;99(16):5749-5752.

81. Vchirawongkwin V, Rode BM, Persson I. Structure and dynamics of sulfate ion in aqueous solution an ab initio QMCF MD simulation and large angle X-ray scattering study. *The Journal of Physical Chemistry B*. 2007;111(16):4150-4155.

82. Maheshwary S, Patel N, Sathyamurthy N, Kulkarni AD, Gadre SR. Structure and stability of water clusters $(H_2O)_n$, n= 8−20: An ab initio investigation. The Journal of Physical Chemistry A. 2001;105(46):10525-37

83. Gaus M, Cui Q, Elstner M. DFTB3: Extension of the Self-Consistent-Charge Density-Functional Tight-Binding Method (SCC-DFTB). *J Chem Theory Comput*. 2011;7(4):931-948.

84. Grabowski SJ. Hydrogen bonding strength—measures based on geometric and topological parameters. *J Phys Org Chem*. 2004;17(1):18-31.

85. Popelier PLA. Characterization of a Dihydrogen Bond on the basis of the Electron Density. *J Phys Chem A*. 1998;102(10):1873-1878.

86. Johnson, S. M., Williams, J. R., & Cook, B. K. Quaternion-based rigid body rotation integration algorithms for use in particle methods. *International journal for numerical methods in engineering*, 2008; *74*(8), 1303-1313.

87. Kitchen, D. B., Hirata, F., Westbrook, J. D., Levy, R., Kofke, D., & Yarmush, M. Conserving energy during molecular dynamics simulations of water, proteins, and proteins in water. *Journal of computational chemistry*, 1990; *11*(10), 1169-1180